Chiral Spaces: Dissymmetric Capsules Through Self-Assembly

José M. Rivera, Tomás Martín, Julius Rebek Jr.*

Molecules with self-complementary surfaces interact through weak intermolecular forces to form assemblies, and the assembled states frequently exhibit distinctive properties. Described here are systems in which symmetrical molecules assemble through hydrogen bonding to produce capsules with dissymmetric cavities. The capsules form and dissipate on a time scale that permits their direct observation by nuclear magnetic resonance measurements, and they act as hosts for smaller molecular guests. Molecular recognition of chiral guests, such as naturally occurring terpenes, determines which dissymmetric cavities are preferentially formed in the assembly process.

Molecule-within-molecule complexes are proving ever more useful in physical organic chemistry. They provide a means of stabilizing reactive intermediates (*1*), observing new forms of stereoisomerism (*2*), accelerating reactions (*3*), and probing the characteristics of the liquid state (*4*). A number of chiral (handed) cavitands such as cryptophanes (*5*, *6*) and carcerands (*7*, *8*) that rely on conventional covalent-bond synthesis in the preparation of their complexes have been described. We describe here the use of weak intermolecular forces to assemble dissymmetric molecule receptacles capable of encapsulating smaller species. The principles of molecular recognition govern which dissymmetric cavities are assembled in the presence of the guest species.

J. M. Rivera, Department of Chemistry, Massachusetts Institute of Technology, Cambridge, MA 02139, USA, and Skaggs Institute for Chemical Biology and Department of Chemistry, Scripps Research Institute, La Jolla, CA 92037, USA.
T. Martín and J. Rebek Jr., Skaggs Institute for Chemical Biology and Department of Chemistry, Scripps Research Institute, La Jolla, CA 92037, USA.
*To whom correspondence should be addressed.

Pseudospherical capsules such as the "softball" (Fig. 1A) assemble through the dimerization of self-complementary subunits in organic solvents (*9*). This self-recognition involves the hydrogen-bond acceptors in the central bicyclic unit and the donors on the terminal glycolurils, and the architecture of the resulting softball tolerates some diversity in the size of the spacers between these elements. For example, either benzene or ethylene can be inserted, and the latter spacer can be used in two different orientations: The endocyclic system gives small pseudospherical capsules, whereas the exocyclic version gives a capsule of larger size (*10*). If two different spacers are used in the same subunit, the subunit still maintains a plane of symmetry and is achiral. Dimerization of the achiral monomer reduces the symmetry, and a chiral capsule results (Fig. 1, B and C) (*11*). The dimeric assembly exists as an equal (racemic) mixture of two mirror-image forms (enantiomers) when the guests inside are symmetrical. The enantiomers can and do interconvert by dissociation and recombination of the subunits. When the guests themselves are chiral, the assemblies are diastereomeric and need not be present in equal amounts. Instead, the populations of the two diastereomers will be determined by whatever molecular recognition exists between the chiral space inside the host and the chiral shape of guest.

Capsules of **1**·**1** and of **2**·**2** have idealized cavities of 241 and 231 Å^3, respectively (*12*), but a variability of ~10% in these values is likely because the "breathing" dynamics of the dimer results in the deformation of hydrogen bonds in the system. These variations in hydrogen-bond directionality and length are generally thought to involve small energy changes, but they provide the system with enough flexibility to potentially undermine the process of molecular recognition. Our experience with these systems is that molecules with the right shape are bound more strongly when their volumes are ~55 ± 9% of the cavity volume (*13*). We undertook the present study to determine whether guests experience intensified sensations of dissymmetry in the highly confined space or if the interior space is too deformable to show selective encapsulating properties.

The syntheses of **1** and **2** were accomplished as shown in Fig. 2 by the stepwise acylation of the hydrazine derivatives **3** (*4*), **4**, and **5** (*10*) with tetraester **6** (*11*) by a procedure similar to that established for the

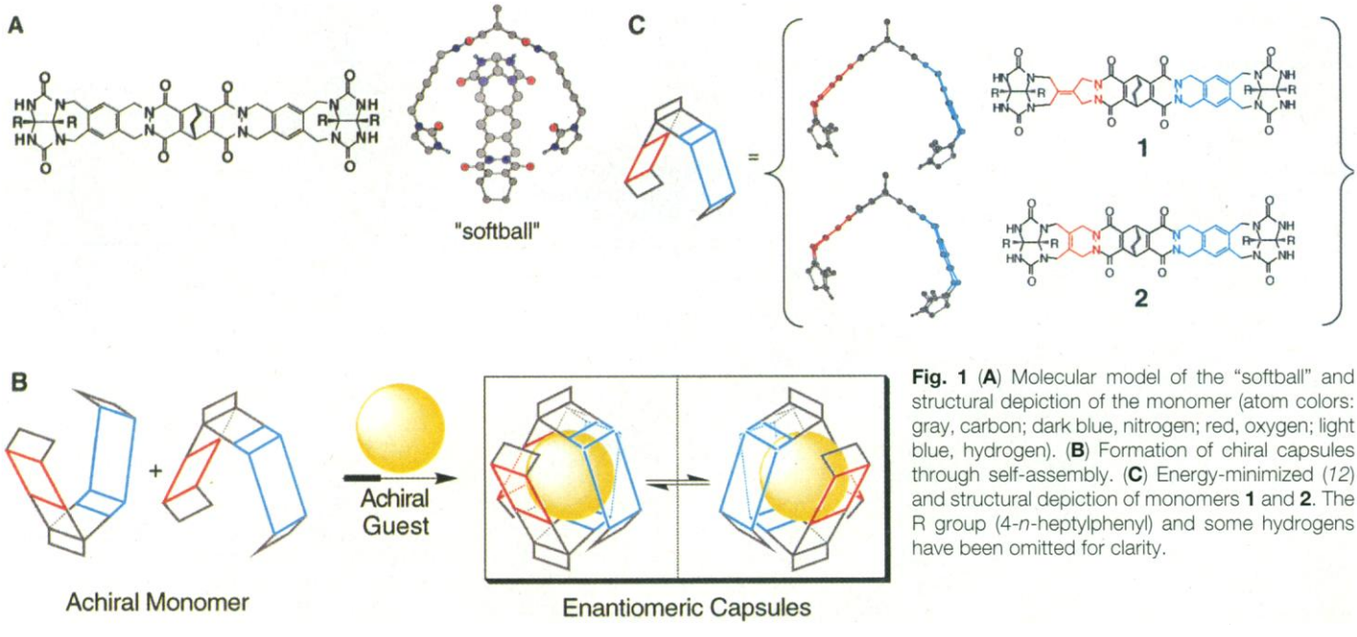

Fig. 1 (**A**) Molecular model of the "softball" and structural depiction of the monomer (atom colors: gray, carbon; dark blue, nitrogen; red, oxygen; light blue, hydrogen). (**B**) Formation of chiral capsules through self-assembly. (**C**) Energy-minimized (*12*) and structural depiction of monomers **1** and **2**. The R group (4-*n*-heptylphenyl) and some hydrogens have been omitted for clarity.

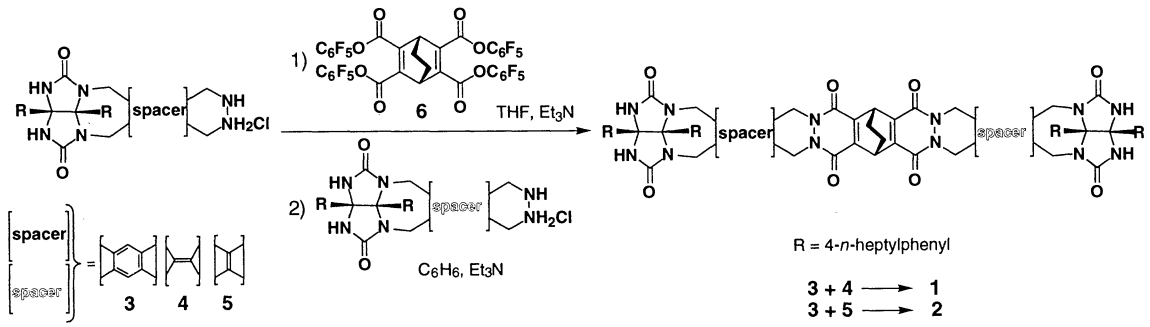

Fig. 2. Synthesis of monomers **1** and **2**. Abbreviations: THF, tetrahydrofuran; Et_3N, triethylamine.

softball. In solvents that are not good guests, such as chloroform-*d*, methylene chloride-d_2, and *p*-xylene-d_{10}, neither **1** nor **2** gave well-defined dimeric assemblies in the absence of nucleating guests, as demonstrated by their broadened ^{1}H nuclear magnetic resonance (NMR) spectra. In solvents such as benzene-d_6 or toluene-d_8, they exhibited the sharp spectra and the downfield N–H resonances characteristic of dimeric assemblies. The latter solvents are good guests themselves (*4*).

Encapsulation studies with chiral guests (Fig. 3) showed the formation of diastereomeric complexes with **1·1** and **2·2**. In the ^{1}H NMR spectra of **1·11·1**, for example, each diastereomer shows four N–H peaks, and the signals for the guest inside are doubled (Fig. 4, A and B). The data summarized in Table 1 show that one of the two possible diastereomeric complexes is formed with some degree of preference (*14*). With a rather small guest such as **7**, no selectivity is observed. However, selectivities increase with the size of the guest, with maximum selectivity being attained with the largest guest, **11**. Selectivities for the same guests are also greater with the smaller **2·2**, where more contact between the guest and inner lining is expected. Ratios of 2:1 can be seen in the ^{1}H NMR spectra for complexes [**1·11·1**] and [**2·11·2**] (Fig. 4, C and D). Our experience with similar systems shows that the presence of guest functional groups capable of hydrogen bonding to the host are as important as the guest's size or shape for selectivity (*10*). In particular, the greatest selectivity is expected for guests that share the C_2 symmetry of the hosts, guests that are of appropriate size to make extensive surface contacts with the hosts, and guests that offer a specific array of hydrogen-bonding sites to interact with the seam of hydrogen bonds that hold the host together. It appears that the host capsules are flexible enough to arrange comfortably around a guest but still maintain enough rigidity to be formed preferentially in the presence of a chiral guest.

Earlier Rebek and associates reported capsules with dissymmetric outer surfaces (*11*) and those with asymmetric cavity linings (*15*). The present work shows that dissymmetric spaces are also accessible through assemblies held together by weak intermolecular forces, and guest enantioselectivity is possible even with the molecular flexibility inherent in this system. The results augur well for access to reaction chambers capable of asymmetric catalysis, as the formation and breakdown of the assemblies take place rapidly at ambient temperatures.

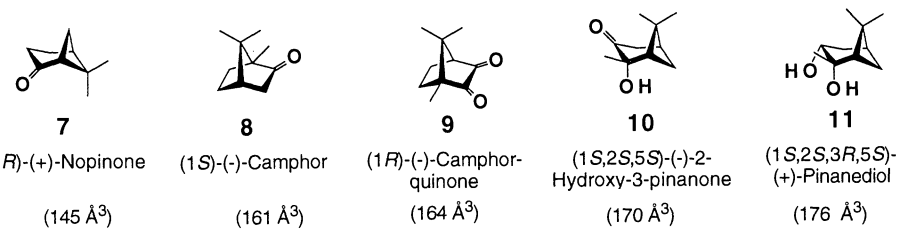

Fig. 3. Structural depiction and names of the chiral guests **7** through **11**. The molecular volumes (in cubic angstroms) are given in parentheses (*12*).

Table 1. Thermodynamic data. Abbreviations: K', apparent association constants; $-\Delta G^0$, free energies of formation; DE, diastereomeric excess; and $\Delta(\Delta G^0)$, calculated differences in stability between diastereomeric complexes of **1·1** and **2·2** with chiral guests in *p*-xylene-d_{10} at 295 K (*14*).

Guest	K'_A (M^{-1})	$-\Delta G^0_A$ (kcal mol^{-1})	K'_B (M^{-1})	$-\Delta G^0_B$ (kcal mol^{-1})	DE (%)	$\Delta(\Delta G^0)$ (kcal mol^{-1})
			Complex **1·1**			
7	630	3.8	620	3.8	0	0
8	1100	4.1	870	4.0	12	0.1
9	960	4.0	850	4.0	6	0.1
10	1200	4.1	800	3.9	19	0.2
11	810	3.9	420	3.5	32	0.4
			Complex **2·2**			
7	290	3.3	270	3.3	0	0
8	420	3.5	300	3.3	17	0.2
9	310	3.4	250	3.2	12	0.2
10	300	3.4	170	3.0	29	0.4
11	390	3.5	190	3.1	35	0.4

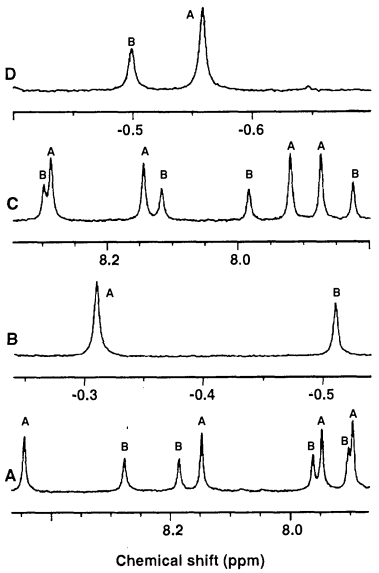

Fig. 4. Sections of ^{1}H NMR (600 MHz) spectra for [**1·11·1**] and [**2·11·2**] in *p*-xylene-d_{10}: (**A**) N–H region for [**1·11·1**]; (**B**) one of the methyl groups of **11** inside **1·1**; (**C**) N–H region for [**2·11·2**]; (**D**) one of the methyl groups of **11** inside **2·2**. The letters A and B represent the predominant and subordinate complexes, respectively.

REFERENCES AND NOTES

1. D. J. Cram, M. E. Tanner, R. Thomas, *Angew. Chem. Int. Ed. Engl.* **30**, 1024 (1991); R. Warmuth, *ibid.* **36**, 1347 (1997).
2. P. Timmerman, W. Verboom, F. C. J. M. van Veggel, J. P. M. van Duynhoven, D. N. Reinhoudt, *ibid.* **33**, 2345 (1994).
3. J. Kang and J. Rebek Jr., *Nature* **385**, 50 (1997).
4. R. Meissner, X. Garcias, S. Mecozzi, J. Rebek Jr., *J. Am. Chem. Soc.* **119**, 77 (1997).
5. J. Canceill, J. Lacombe, A. Collet, *ibid.* **107**, 6993 (1985).
6. J. Costante-Crassous, T. J. Marrone, J. M. Briggs, J. A. McCammon, A. Collet, *ibid.* **119**, 3818 (1997).
7. J. K. Judice and D. J. Cram, *ibid.* **113**, 2790 (1991); J. Yoon and D. J. Cram, *ibid.* **119**, 11796 (1997).
8. For additional examples of chirality through self-assembly, see: M. J. Brienne *et al.*, *Tetrahedron Lett.* **35**, 8157 (1994); A. Bilyk and M. M. Harding, *J. Chem. Soc. Chem. Commun.* **1995**, 1697 (1995); J. Sánchez-Quesada, C. Seel, P. Prados, J. de Mendoza, *J. Am. Chem. Soc.* **118**, 277 (1996); S. B. Lee and J.-I. Hong, *Tetrahedron Lett.* **37**, 8501 (1996); T. Mizutani, S. Yagi, A. Honmaru, H. Ogoshi, *J. Am. Chem. Soc.* **118**, 5318 (1996); E. E. Simanek, S. Qiao, I. S. Choi, G. M. Whitesides, *J. Org. Chem.* **62**, 2619 (1997); L. R. MacGillivray and J. L. Atwood, *Nature* **389**, 469 (1997).
9. R. S. Meissner, J. Rebek Jr., J. de Mendoza, *Science* **270**, 1485 (1995).
10. J. M. Rivera-Ortiz, T. Martín, J. Rebek Jr., *J. Am. Chem. Soc.*, in press.
11. Y. Tokunaga and J. Rebek Jr., *ibid.*, *J. Am. Chem. Soc.* **120**, 66 (1998).
12. We performed molecular modeling using MACROMODEL 5.5 (Amber* force field): F. Mohamadi *et al.*, *J. Comput. Chem.* **11**, 440 (1990). The volumes for the guests and the cavities were obtained from the GRASP program [A. Nicholls, K. A. Sharp, B. Honig, *Proteins* **11**, 281 (1991)].
13. S. Mecozzi and J. Rebek Jr., *Chem. Eur. J.*, in press.
14. We obtained all measurements by ^{1}H NMR experiments using the integrals for the peaks of the guest inside and outside the capsules. There is an estimated 10% error in these measurements. The equilibrium may be described as follows:

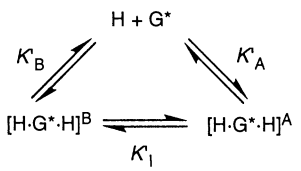

The following assumptions were made: (i) the amount of dimer (unfilled or filled with solvent) present before addition of the guest is negligible; (ii) after addition of the guest, all of the host material not assembled into the capsule is in the aggregate state; and (iii) the association of the guest with itself is negligible.

$$K'_A = \frac{[H\cdot G^*\cdot H]^A}{[H][G^*]} = \frac{aV}{[h - 2(a + b)][g - (a + b)]} \quad (1)$$

$$K'_B = \frac{[H\cdot G^*\cdot H]^B}{[H][G^*]} = \frac{bV}{[h - 2(a + b)][g - (a + b)]} \quad (2)$$

$$K'_I = \frac{[H\cdot G^*\cdot H]^A}{[H\cdot G^*\cdot H]^B} = \frac{K'_A}{K'_B} \quad (3)$$

$$\Delta(\Delta G^0) = -RT \ln K'_I \quad (4)$$

$$a = g(I_{gA}/I_{gT}) \quad (5)$$

$$b = g(I_{gB}/I_{gT}) \quad (6)$$

$$I_{gT} = I_{gO} + I_{gA} + I_{gB} \quad (7)$$

where K'_A and K'_B are the apparent association constants for the predominant and the subordinate complexes, respectively, and K'_I is the apparent isomerization constant between the two complexes. In these equations H is the host; G* is the chiral guest; $[H\cdot G^*\cdot H]^A$ and $[H\cdot G^*\cdot H]^B$ are the concentrations of the predominant and the subordinate complexes, respectively: ΔG^0 is the free energy of formation; T is temperature; and R is the ideal gas constant; I_{gT} is the sum of all the integrals corresponding to the guest (subscript T stands for total); I_{gO} is the integral for the signal of the guest outside the capsule, I_{gA} is the integral for the signal of the guest in complex A; I_{gB} is the integral for the signal of the guest in complex B; h is the initial amount of monomer (in millimoles); g is the amount (in millimoles) of guest added to the solution; a is the amount of guest (in millimoles) in complex A; b is the amount of guest (in millimoles) in complex B; and V is the total volume (in milliliters).

15. R. K. Castellano, B. H. Kim, J. Rebek Jr., *J. Am. Chem. Soc.* **119**, 12671 (1997).

16. This research was supported by the Skaggs Research Foundation and NIH. We thank U. Obst for advice on molecular dynamics studies. Administración de Fomento Económico of Puerto Rico provided fellowship support to J.M.R. The Ministerio de Educación y Cultura of Spain provided fellowship support to T.M.

13 November 1997; accepted 7 January 1998

Chain Reactions Linking Acorns to Gypsy Moth Outbreaks and Lyme Disease Risk

Clive G. Jones,* Richard S. Ostfeld, Michele P. Richard, Eric M. Schauber, Jerry O. Wolff

In eastern U.S. oak forests, defoliation by gypsy moths and the risk of Lyme disease are determined by interactions among acorns, white-footed mice, moths, deer, and ticks. Experimental removal of mice, which eat moth pupae, demonstrated that moth outbreaks are caused by reductions in mouse density that occur when there are no acorns. Experimental acorn addition increased mouse density. Acorn addition also increased densities of black-legged ticks, evidently by attracting deer, which are key tick hosts. Mice are primarily responsible for infecting ticks with the Lyme disease agent. The results have important implications for predicting and managing forest health and human health.

Oak trees (*Quercus* spp.) produce large autumnal acorn crops (masting) every 2 to 5 years, producing few or no acorns during intervening years (*1–4*). Acorns are a critical food for white-footed mice, *Peromyscus leucopus* (*1*, *4–6*). Mice are important predators of pupae of the gypsy moth, *Lymantria dispar* (*1*, *6–10*). This introduced insect periodically undergoes outbreaks (*11*, *12*) that defoliate millions of hectares of oak forests, decreasing tree growth, survival, and mast production (*13*). An abundance of acorns draws white-tailed deer, *Odocoileus virginianus*, into oak forests (*14*, *15*). Mice and deer are the primary hosts of the black-legged tick, *Ixodes scapularis*, which is the vector of spirochete bacteria (*Borrelia burgdorferi*) that cause Lyme disease in humans (*16–18*). Here we report the results of experimental removal of mice and addition of acorns, which demonstrate how acorn production is connected to gypsy moth outbreaks and Lyme disease risk.

Masting is associated with increased survival and breeding of mice in winter and spring (*19*), with peak densities occurring the following midsummer (*1*, *4*, *6*). High mouse density correlates with high predation rates on moth pupae (*1*, *6*), which may prevent low-density moth populations from increasing (*1*, *6–8*). Conversely, mast crop failure correlates with low mouse densities and low rates of pupal predation the following summer (*1*, *4*, *6*), which may initiate moth outbreaks (*7*, *9*).

Moth populations at our research site reached peak densities in 1990, declined by four orders of magnitude to 0.2 egg masses ha^{-1} by 1992, and remained between 6 and 38 egg masses ha^{-1} in 1993–1994 (*1*). A large red oak (*Q. rubra*) acorn crop in autumn 1994 led to high mouse densities in summer 1995 (*1*). We took advantage of low moth and high mouse densities to remove mice during moth pupation, testing the chain of interactions linking acorns to mice to moths. Mice were removed from three grids of approximately 2.7 ha but were left unmanipulated on three control grids (*20*). Mouse densities did not differ between control and experimental grids in June 1995, just before mouse removal (Fig. 1; $P = 0.18$, paired t test) (*21*). Continuous live trapping reduced mouse densities on experimental grids to less than half those on control grids by the midpoint of a 32-day removal period in June–July coincident with female moth pupation (Fig. 1; $P =$

C. G. Jones, R. S. Ostfeld, M. P. Richard, Institute of Ecosystem Studies (IES), Post Office Box AB, Millbrook, NY 12545, USA.
E. M. Schauber, IES and Department of Ecology and Evolutionary Biology, University of Connecticut, Storrs, CT 06269–3042, USA.
J. O. Wolff, Department of Fisheries and Wildlife, Oregon State University, Corvallis, OR 97331, USA.

*To whom correspondence should be addressed. E-mail: clivegjones@compuserve.com